Flexible Soft Frequency Reuse schemes for heterogeneous networks (macrocell and femtocell)

Chrysovalantis Kosta, Ali Imran, Atta U. Quddus and Rahim Tafazolli
Center of Communication System Research (CCSR),
University of Surrey
Guildford, GU27XH, Surrey, United Kingdom
{c.kosta a.imran, a.quddus, r.tafazolli}@surrey.ac.uk

***Abstract*—A mass deployment of femtocells is anticipated to affect a number of areas more adversely, especially in the cell-edge of the macrocell network. In this paper, we propose a flexible frequency-partitioning scheme for OFDMA network based on cyclic difference sets. The cyclic property of these sets allows a quick construction of orthogonal patterns for the macrocell and femtocell networks with an emphasis on tri-sector sites. The impact and the co-deployment of femtocells is also investigated. Unlike, with existing works in the literature, the novel scheme can adaptively control the level of coverage in the cell-edges areas and additionally enables coexistence of femtocells in the network. Simulation results confirm the effectiveness of the proposed scheme in both macrocell and femtocell networks compared to the legacy soft frequency reuse and universal frequency reuse.**

Keywords-Cyclic difference set; Frequency Partitioning; Inter-cell Interference Coordination; Interference Mitigation schemes

I. INTRODUCTION

The exponential growth of multimedia content on the Internet over the past decade has set out new ambitious targets to meet the ever-increasing demand of user capacity in emerging wireless communication systems [1]. However, the inherent impairments of communication channels particular in indoor environments pose constant challenges to meet the envisioned targets. On the other hand, due to the high cost and scarcity of wireless spectrum, achieving a high spectral efficiency is crucial. As a result, a higher area spectral efficiency through a tighter spectrum reuse is highly desirable in the cellular systems. However, this inevitably leads to Inter-Cell Interference (ICI).

Recently, several interference mitigation schemes have been proposed in literature to address this problem. According to the 3GPP studies [2], the ICI mitigation can be divided into three main classes: 1) ICI randomization, 2) ICI cancellation, and 3) ICI Coordination/Avoidance (ICIC). In the first class the interference is averaged across the whole spectrum via spreading sequences (e.g. scrambling and interleaving), and therefore is not actually cancelled out. By contrast, in the second class, the interference is successfully suppressed by using advanced signal processing techniques. Although these techniques are becoming popular, however, the complexity at the receiver side is still a challenging issue particularly in the presences of multiple dominant interferes. ICIC techniques, on the other hand, present pragmatically a more feasible solution to mitigate the interference via orthogonalization of wireless resources across subsets of users that are severely impacted by the interference. This orthogonalization can be achieved through static or dynamic spectrum allocation. The dynamic spectrum allocation has the potential to yield higher spectrum reuse efficiency compared with the static, however, at the cost of additional inter-cell signaling and complexity.

With advent of femtocell deployment that aims to both extend the radio coverage in a licensed band and provide a large number of bandwidth-hungry multimedia services, the ICIC techniques have become more challenging and more important than ever [3]. In this paper, our focus is to address this spectrum-sharing challenge in the heterogeneous networks through low-complexity algorithm that allows the quick construction of orthogonal patterns for macrocell network with emphasis on tri-sectorized cellular systems.

Traditionally, the ICI in conventional cellular systems was managed by a common clustering technique, also known as Integer Frequency Reuse (IFR) [4]. Two classical IFR schemes are Frequency Reuse 1 (FR1) and Frequency Reuse 3 (FR3). The former scheme is well known as universal frequency reuse, where the entire frequency spectrum is reused over all cells. However, by employing this scheme only the users close to the base station experience good channel quality whereas the far-off users suffer from low radio conditions due to severe ICI. Contrarily, in the latter scheme, the received signal quality of all users is enhanced; however, on the other hand the spectral efficiency of each cell is reduced by a Frequency Reuse Factor (FRF). Figure 1 illustrates how the power-frequency resource restrictions are applied at each cell in FR3 scheme as opposed to FR1 scheme. It is important to note that the FRF of IFR technique is restricted by a list of integer numbers: {1, 3, 4, 7, …, $i^2 + i \cdot j + j^2 \mid i, j \in N$}.

Another drawback of the IFR technique is that higher spectrum reuse efficiency always causes a steep degradation on spectrum efficiency. This problem is addressed by a reuse-partitioning scheme, also known as Fractional Frequency Reuse (FFR) [5]. The employment of FFR in ICIC techniques marked a significant improvement as it compromises the accessible frequency resource to a lesser extent. The rationale behind FFR lies in the fact that the users at the cell borders experience worse radio conditions compared to those in the center of the cell. Therefore, it is logical to use different levels of FRF for users in each sub-cell area, such that a higher FRF for the cell-edge area and a lower FRF for the cell-center area.

This work has been performed in the framework of the ICT project ICT-4-248523 Be-FEMTO, which is partly funded by the European Union

978-1-4244-8331-0/11/$26.00 ©2011 IEEE

Two important variants of FFR technique are Partial Frequency Reuse (PFR) [5] and Soft Frequency Reuse (SFR) [7] as shown in Fig. 2 and Fig. 3, respectively. In this paper, we exploit the fact that, theoretically, there is no limitation on the number of sub-cell (or concentric tiers) to cover a cell area. For example, the authors in [9] defined three geographically non-overlapping users groups corresponding to three concentric tiers.

As mentioned above, one of the main drawbacks of existing IFR techniques is that the FRF is limited within a list of integer numbers. For this reason, a flexible scheme is proposed in [8], and further extended in [9] based on a principle of cyclic difference set from information theory, which the FRF can use a non-integer numbers such as 7/3 or 7/4. It is found that their employment in ICIC has potentially a high value, since it introduces a high degree of orthogonalization with a low mathematical complexity among adjacent cells.

Our main contribution is the employment of a novel (1,2,6)–difference set which shows high orthogonalization in the case of a trisectorized cellular topology. Additionally, unlike most of the existing works, we propose a power adaptation scheme and investigate the performance of SFR scheme using a multi-tier deployment approach where the cell area is divided up to four distinct sub-cell regions. Thus, this region-based arrangement allows not only to control the degree of coverage but also to flexibly tune the service among these regions. Besides this, we extend our framework to enable a plug-and-play deployment of femtocells in the existing cellular network.

The rest of the paper is organized as follows. In Section II, we describe briefly the relevant theory of cyclic difference set and we present the proposed FSFR scheme. Then in Section III, a simulation study is carried out to investigate the effectiveness of the proposed scheme and finally with Section IV we conclude this paper.

II. Proposed Scheme

As explained above, the ICIC or alternatively, the orthogonalization of wireless resources is achieved by applying restrictions on frequency/time domain. In fact, this approach can be generalized using some fundamental principles of mathematics. This gives us the motivation to investigate a popular technique, which generates orthogonal patterns in a low complexity manner, e.g. the cyclic difference set.

A. Cyclic difference sets

Definition 1: ([10] pp.261) Let a set $\Gamma = \{0, 1, 2, ..., \upsilon\text{-}1\}$ of order υ and a non-empty set ($D \neq \emptyset$) of order k. If $D \subset \Gamma$ such as $0 < k < \upsilon$, then the set $D=\{d_0, d_1, d_{k-1}\}$ is called a cyclic (υ, κ, ζ) – difference set if it satisfies a list of operational differences of the congruent $d_i - d_j \equiv t \pmod{\upsilon}$ for each two different non-zero elements of Γ (d_i, d_j, $\in D$, $d_i \neq d_j$) and for each $1 \leq t \leq \upsilon - 1$ precisely ζ times.

Lemma 1: (Symmetry property) A necessary condition for a given D to be a cyclic (υ, κ, ζ)–difference set in a group Γ, is:

$$\zeta \cdot (\upsilon - 1) = \kappa^2 - \kappa \qquad (1)$$

Lemma 2: (Difference property set) If D is a cyclic (υ, κ, ζ)–difference set in a group Γ, let a constant $\gamma \in \Gamma$ to be added to each of its element, thus the new set $D' = D + \gamma = \{d_0 + \gamma, d_1 + \gamma, d_{k-1} + \gamma\} \pmod{\upsilon}$ is also a symmetric set of (υ, κ, ζ).

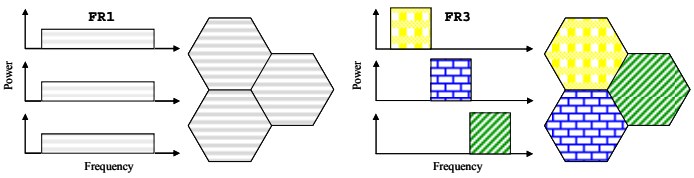

Figure 1. Examples of IFR technique – FR1 & FR3 schemes

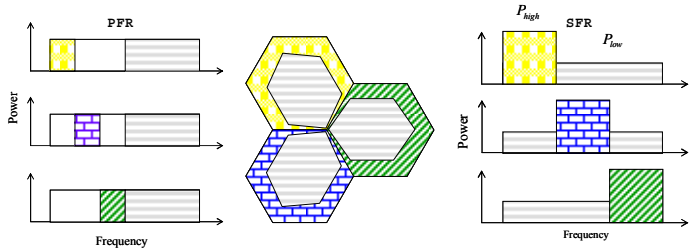

Figure 2. Partial Frequency Reuse (PFR) & Soft Frequency Reuse (SFR)

Lemma 3: Precisely ζ common elements can be found between any two subsets such as $D_1, D_2 \in D'$ ($D_1 \neq D_2$).

For instance, two arbitrary members of cyclic (7,3,1)-difference set are (1,2,4)–difference set and (1,2,6)– difference set. Both satisfy above lemmas; however, in this study we found that the use of latter difference set enhances the orthogonalization of wireless resources through the tri-sectorized cell-sites to a greater extent than the former, and therefore its employment in ICIC techniques is favorable. Next, by using the *difference property,* six symmetric subsets are extracted as follows: (2,3,0), (3,4,1), (4,5,2), (5,6,3), (6,0,4) and (0,1,5). Last, we note that the repetition of each element of a symmetric subsets of the (7,3,1)-difference set is precisely one.

B. Employment of sequences of (1,2,6)-difference set

Here, we define the following sequences that are element wise cyclic left shifted:
Seq1:{(1,2,6),(2,3,7), (3,4,1), (4,5,2), (5,6,3), (6,7,4), (7,1,5)}
Seq2:{(6,1,2),(7,2,3), (1,3,4), (2,4,5), (3,5,6), (4,6,7), (5,7,1)}
Seq3:{(2,6,1),(3,7,2), (4,1,3), (5,2,4), (5,3,1), (7,4,6), (1,5,7)}
Note that for notational simplicity, the element 0 is substituted with 7.

The main reasoning behind this deployment is illustrated in Figure 4. Each of the above sequence has seven symmetric subsets – i.e. 21 elements – and therefore it yields exact allocation for the case of a tri-sectored one–tier network layout – i.e. 21 sectors. According to the frequency restriction diagram as shown in Figure 4(a), each subset with same element is required to satisfy a minimum reuse distance in an appropriate angle. An example of resource allocation with respect to the frequency restriction diagram of an above-mentioned sequence – i.e. Seq1 – is shown in Figure 4(b). For illustration simplicity, henceforth a hexagon represents a tri-sectorized cell site.

C. Flexible SFR (FSFR) Scheme

In this subsection, we introduce novel variants of SFR schemes to allow more flexible reuse of the available spectrum.

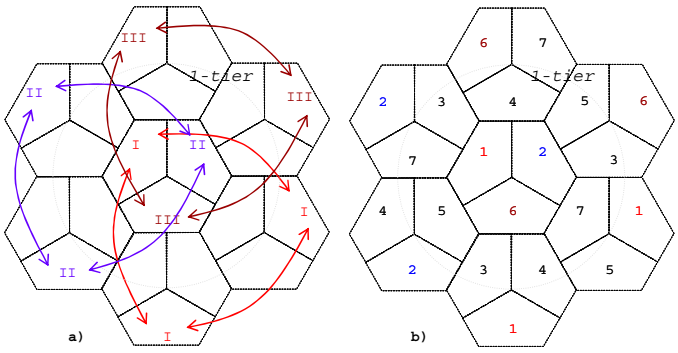

Figure 4. Frequency Restriction Diagram

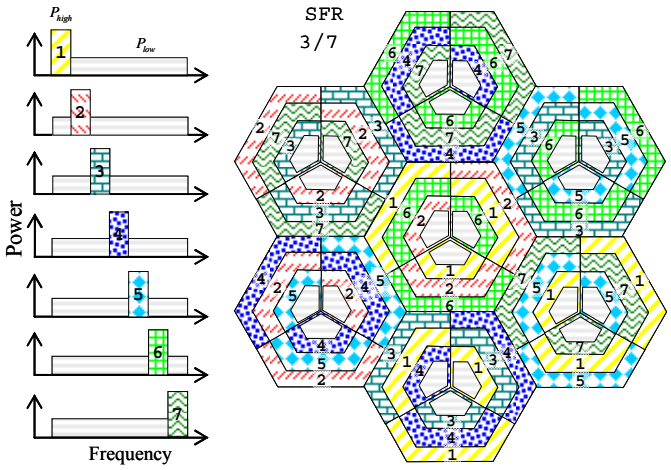

Figure 5. SFR 3/7 scheme.

TABLE I. POWER ADAPTATION SCHEME FOR FSFR

Scheme	P_{high}	P_{low}	Cell diagram
SFR 1/7	α	$\frac{7-\alpha}{6}$	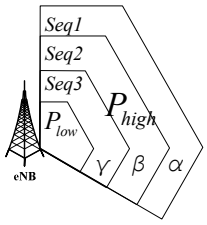
SFR 2/7	α, β	$\frac{7-\alpha-\beta}{5}$	
OFP 2/7			
SFR 3/7	α, β, γ	$\frac{7-\alpha-\beta-\gamma}{4}$	

Figure 5 illustrates an instance of the proposed scheme. Instead of having only a tier on top of the cell-edge region, it is possible to form up to three virtual tiers each using a different part of spectrum. Following the same concept, other similar variants, can be defined as shown in Table I. For each defined SFR variant, i.e. SFR x/7 (x∈ {1,2,3}), a set of parameters that can be used to control the level of high-transmit power (P_{high}) versus low-transmit power (P_{low}), are defined as power amplification factors (α, β, γ). For illustration purposes, a detailed cell diagram is drawn as shown in Table I, where in each tier a power amplification factor is associated with the corresponding sequence as defined above. In this way, the new scheme allows not only to control the degree of coverage but also to flexibly tune the service between the cell-edge and cell-center regions. Since the femtocell deployment is anticipated to affect a number of areas more adversely particularly in cell-edge regions, an additional variant of SFR is proposed i.e. Orthogonal Frequency Pattern (OFP) 2/7 to further enhance the mitigation in these affected areas. This scheme is similar to SFR 2/7, except for the fact that a fraction of spectrum is exclusively reserved for femtocells – i.e. Seq3.

III. SIMULATION STUDY

A. *Topology of eNB & HeNB networks*

This study considers active data transmission only in the downlink direction in the context of OFDMA (Orthogonal Frequency-Division Multiple Access), targeting 3GPP LTE (Long Term Evolution). We consider a cellular layout of a 19-cell with three 120-degree sectorized antennas where each cell contains an eNB (LTE eNodeB) in its center. Next, for HeNB (LTE Home eNB) deployment, each house is modeled as a square block with dimension 10x10. Inside of each block, both HeNB and FUE (Femto UE) are dropped according to the uniform distribution. However, a fixed number of blocks and UEs (User Equipment) are placed in each cell (ref. Table II). Further, to eliminate the boundary effect a wrap-around technique is adopted and therefore the Signal-to-Interference plus Noise Ratio (SINR) is calculated including all the interferers. Additionally, we assume that the HeNB deployment is isolated from the eNB by an external wall. The main simulation parameters for this study are listed Table II.

B. *Effective Spectral Efficiency*

We evaluate the performance of existing and proposed schemes using the metric called ESE (Effective Spectral Efficiency in bps/Hz/cell) as proposed in our earlier work [12]. The motivation of this metric is that the ESE not only reflects both the spectral efficiency and spectrum reuse efficiency in a holistic way but also incorporates the outage effects. The calculation of ESE is described as follows: The network area is divided in virtual bins of same size. The geometric SINR in each bin is calculated by assuming that the system is fully loaded – i.e. each of the frequency resource is allocated to each cell. As shown in the Table III, a lookup table maps all-possible CQI values with a Modulation & Coding Scheme, Spectral Efficiency (SE), and SINR threshold over a defined quality control measurement of 10% BLER (BLock Error Ratio) [11]. The ESE is then expressed as follows:

$$ESE = \frac{1}{FRF} \sum_{l=0}^{L} \frac{A_l}{A_t} \times SE_l \qquad (2)$$

where A_l is the aggregate area of bins where each user has reported same received signal quality (or CQI parameter), A_t is the total area of bin in the coverage area, FRF is the frequency reuse factor and L is the total number of CQI values that a UE may report. Note that for LTE systems L=16, including CQI = 0.

Additionally, in order to evaluate the performance thoroughly within the cell area, an extension of ESE – i.e. Radial Expected Spectral Efficiency (RESE) – is defined as follows:

$$RESE(r_1, r_2) = \frac{1}{\text{FRF}} \sum_{l=0}^{L} \frac{A_l(r_1, r_2)}{A_t} \times SE_l \qquad (3)$$

Here, $A_l(r_1,r_2)$ represents the percentage of bins between the concentric tiers denoted by cell radius r_1 and cell radius r_2.

C. Simulation Results & Analysis

In this subsection, based on the aforementioned assumptions and metrics, we evaluate the performance of the proposed FSFR (SFR x/7 and OFP 2/7) scheme against the benchmarks of IFR 1 (FR1) and legacy SFR (SNR 1/3). We divide entire cell area into the cell-center and cell-edge regions in proportion to the amount of available resource for each region. Furthermore, to examine the ESE performance, we define RESE (70,100) and RESE (0,100) as cell-edge ESE and sector ESE, respectively. We assume that the overlapping areas between adjoining cells are concentric rings of cell radius 70 % up to 100% thus the RESE(70,100). In each cell, the schedule resource unit can be selected based either on user-path gain or user geometry. As the latter performed best, only these results are presented. The rest of simulation parameters such as power amplification factors and the percentage of the cell-center region are given in Table IV.

As mentioned above, only the OFP 2/7 scheme has a reserved frequency band for the FUE. For the rest of the schemes, we apply the following simple interference mitigation strategy while deploying HeNBs: For schemes, with two or more concentric tiers– i.e. SFR 1/3 and SFR x/7 – the HeNB reuses the fraction of bandwidth used in the cell-center region if it located at cell-edge region and vice versa. For evaluation purposes, the rest of the schemes i.e. FR1, the HeNB employs randomly half of the entire spectrum.

Table V shows the performance of the eNB and HeNB deployment obtained through system-level simulation in terms of ESE. In the case of eNB, it can be seen that although the universal frequency reuse scheme has the highest sector ESE, its cell-edge ESE performance is not satisfactory. The SFR 1/3 and proposed SFR x/7 schemes have slightly lower sector ESE compared with FR1, however, the cell-edge performance is generally better for these schemes. On the other hand, the OFP 2/7 scheme shows generally a lower sector ESE (in both eNB and HeNB) due to the higher reuse factor i.e. 7/6 (1/7 is reserved for HeNB deployment). This loss is noticeable by comparison of the SFR 2/7 and its variant the OFP 2/7.

It is worth to note that the proposed SFR x/7 schemes, the performance in both cell-edge eNB ESE and average HeNB ESE is gradually increased with the number of concentric tiers in the cell-edge area while the sector eNB ESE remains almost the same. Consequently, the SFR 3/7 scheme with three tiers in the cell-edge area outperforms all other schemes in terms of cell-edge eNB ESE and average HeNB ESE.

The percentage of sector ESE Loss indicates the degradation in ESE (bps/Hz/cell) of each eNB sector over the HeNB deployment. The FR1 has a high mean HeNB ESE performance; however, the sector ESE loss experienced in this scheme is quite high. As it can be seen, the legacy SFR and SFR x/7 schemes show a relatively smaller loss when compared to FR1 scheme since the FUEs refrain from locally

TABLE II. LIST OF MAIN SIMULATION PARAMETERS

Parameters	Values
Total Bandwidth	20 MHz
No of Physical Resource Blocks (PRBs)	100 PRBs
Total bandwidth per PRB	180KHz
Site-to-Site Distance	500 m
Antenna model	Berger
eNB Power	43 dBm
HeNB Power	20 dBm
Main fading loss parameter	Path loss model
Outdoor path loss model	$L = 128.1 + 37.6 \log_{10} D$
Indoor path loss model	$L = 127 + 30 \log_{10} D$
External wall loss	10dB
Inter-distance of UEs	1 per $15m^2$
Inter-distance of Houses	1 per $41m^2$

TABLE III. SE MAPPED WITH SINR THRESHOLD (10% BLER) [11]

CQI No	Modulation & Coding Scheme		Spectral Efficiency (bps/Hz)	SINR Threshold
1	QPSK	78/1024	0.1523	-6.94 dB
2	QPSK	120/1024	0.2344	-5.14 dB
3	QPSK	193/1024	0.3770	-3.18 dB
4	QPSK	308/1024	0.6016	-1.25 dB
5	QPSK	449/1024	0.8780	0.76 dB
6	QPSK	602/1024	1.1758	2.67 dB
7	16QAM	378/1024	1.4766	4.69 dB
8	16QAM	490/1024	1.9141	6.52 dB
9	16QAM	616/1024	2.4063	8.57 dB
10	64QAM	466/1024	2.7305	10.36 dB
11	64QAM	567/1024	3.3223	12.29 dB
12	64QAM	666/1024	3.9023	14.17 dB
13	64QAM	772/1024	4.5234	15.88 dB
14	64QAM	873/1024	5.1152	17.81 dB
15	64QAM	948/1024	5.5547	19.83 dB

TABLE 4. LIST OF OTHER SIMULATION PARAMETERS

Scheme		Percentage (%) of cell-center area	Power Amplification Factor		
			α	β	γ
FR 1		N/A	N/A	N/A	N/A
SFR 1/3		2/3	1.9	N/A	N/A
FSFR	SFR 1/7	6/7	3.0	N/A	N/A
	SFR 2/7	5/7	2.6	1.6	N/A
	SFR 3/7	4/7	2.4	1.6	1.2
	OFP 2/7	5/7	2.6	1.6	N/A

reusing the same spectrum with the UEs. Contrarily to abovementioned SFR schemes, in the case of OFP 2/7 scheme, this loss is almost negligible, since the employment of an orthogonal reuse pattern from femtocell network creates less interference towards the macro network.

Figure 4 depicts the performance of RESE of eNB for different schemes. Note that although the outcome of RESE is through two cell-radial numbers i.e. r_1, r_2 the abscissa shows only the mean value – the offset is set at 2.5. The tradeoff between the spectrum efficiency and spectrum reuse efficiency is more clearly noticeable in the case of the cell edge. As expected, all schemes except FR1 have better cell-edge

TABLE V. ESE RESULTS FOR ENB AND HENB DEPLOYMENT

Scheme		Sector ESE (eNB) (bps/Hz/cell)	Cell-edge ESE (eNB) (bps/Hz/cell)	Average HeNB ESE (bps/Hz/cell)	% of sector ESE Loss (bps/Hz/cell)
FR1		1.67	0.64	1.35	4.86%
SFR 1/3		1.49	1.00	1.93	1.91%
FSFR	SFR 1/7	1.50	0.81	1.07	1.35%
	SFR 2/7	1.49	0.99	1.73	1.75%
	SFR 3/7	1.50	1.10	2.02	1.55%
	OFP 2/7	1.40	1.00	0.62	0.16%

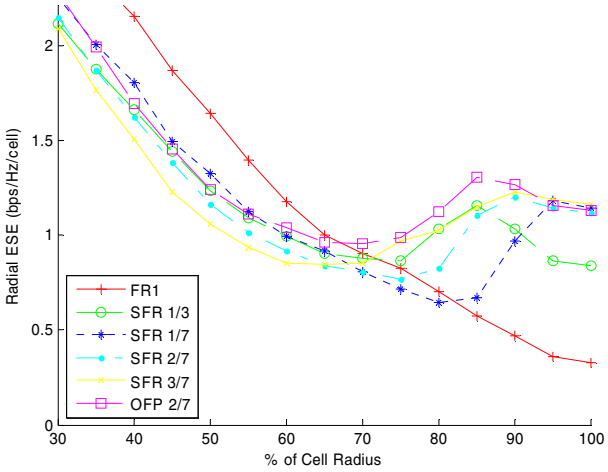

Figure 4. Radial ESE of each scheme of eNB deployment

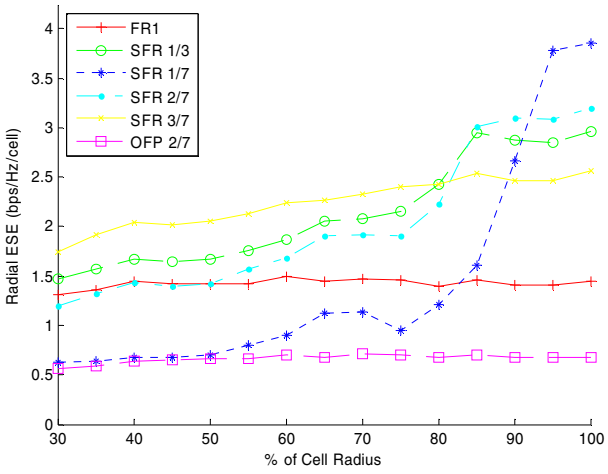

Figure 5. Radial ESE of each scheme of HeNB deployment

performance because of the avoidance scheme through power-frequency inter-cell arrangements. Furthermore, it can be observed as well how the power amplification scheme adjusts the coverage of SFR x/7 schemes between the cell-edge and the cell-center region.

Similarly, the Fig. 5 depicts the RESE performance of HeNB network for different schemes. It can be seen that for schemes with multiple distinct regions (except OFP 2/7), the ESE is higher as the HeNB located at cell edge can employs a wider range of cell-center spectrum. In case of OFP 2/7 and FR1 scheme, the RESE performance is uniform across the whole cell area due to the fixed number of allocated resources to HeNB.

IV. CONCLUSIONS

A novel frequency-partitioning scheme for heterogeneous network based on difference sets is presented in this paper. According to cyclic property of these sets, a quick construction of orthogonal patterns is allowed for the macrocell and femtocell network with emphasis on tri-sector sites. Furthermore, a power adaptation scheme in which can effectively control the level of coverage between the cell-edge and cell-center region is been devised.

The simulation analysis of the proposed scheme is carried out by using a new performance metric called effective spectrum efficiency that provides a valuable insight into the tradeoffs coupled with spectral efficiency and spectrum reuse efficiency. It is observed that proposed flexible scheme achieves not only an enhanced cell-edge spectral efficiency, but also minimal degradation of a forthcoming femtocell deployment through scheme adaptation.

ACKNOWLEDGMENT

This work has been performed in the framework of the ICT project ICT-4-248523 Be-FEMTO, which is partly funded by the European Union. The authors would like to express their gratitude to Mehrdad Shariat and Dua Idris from the BeFEMTO consortium for their reviews and useful comments.

REFERENCES

[1] Femto Forum, http://www.femtoforum.org

[2] 3GPP TR 25.814 v.7.1.0, “Physical layer aspects for Evolved UTRA”, Sep 2006.

[3] A. Quddus, T. Guo, M. Shariat, B. Hunt, A. Imran, Y. Ko, and R. Tafazolli, “Next generation femtocells: An enabler for higher efficiency Multimedia Transmission”, *IEEE Comsoc. MMTC Letter*, vol. 5, no. 5, pp. 27–31, Sep 2010.

[4] P. Godlewski, M. Maqbool, and M. Coupechoux, “Analytical evaluation of various frequency reuse schemes in cellular OFDMA networks,” *in perso.telecom-paristech.fr*, 2008.

[5] M. Sternad, T. Ottosson, A. Ahlen, A. Svensson, “Attaining both coverage and high spectral efficiency with adaptive OFDM downlinks”, *VTC2003-Fall*, Orlando, FL, Oct 2003.

[6] 3GPP R1-050738, Siemens, “Interference mitigation – Considerations and Results on Frequency Reuse”, TSG-RAN WG1 Meeting #42 London, UK, Sep 2005.

[7] 3GPP R1-050507, Huawei, “Soft frequency reuse scheme for UTRAN LTE”, TSG RAN WG1 Meeting #41, Athens, Greece, May 2005.

[8] Y.J. Choi, C.S. Kim, S. Bahk, "Flexible Design of Frequency Reuse Factor in OFDMA Cellular Networks”, *IEEE ICC '06,* vol.4, pp.1784-1788, Jun 2006 .

[9] A. Najjar, N. Hamdi and A. Bouallegue, “Fractional Frequency Reuse Scheme With Two and Three Regions For Multi-cell OFDMA Systems”, *17th TELFOR 2009*, Serbia, Belgrade, Nov 2009.

[10] T. Hellesth, D. Jungnickel, A. Pott and P. Kumar, “Difference sets, Sequences and their Correlation Properties”, *Kluwer Academic Publisher*, 1998.

[11] C. Mehlführer, M. Wrulich, J. C. Ikuno, D. Bosanska and M. Rupp, “Simulating the Long Term Evolution Physical Layer”, *In Proc. of the 17th EUSIPCO 2009*, Glasgow, Scotland, Aug 2009.

[12] A. Imran and M. A. Imran and R. Tafazolli, “A New Performance Characterization Framework for Deployment Architectures of Next Generation Distributed Cellular Networks”, *In Proc. of IEEE PIMRC 2010*, Istanbul, Turkey, Sep 2010.